

The Effect of the Disorder on the Longitudinal Resistance of a Graphene p-n Junction in Quantum Hall Regime

Jiang-chai Chen¹, T. C. Au Yeung², and Qing-feng Sun^{1,*}

¹*Beijing National Lab for Condensed Matter Physics and Institute of Physics,
Chinese Academy of Sciences, Beijing 100190, China*

²*School of Electronic and Electrical Engineering,
Nanyang Technological University of Singapore, 639798, Singapore*

The longitudinal resistances of a six-terminal graphene p-n junction under a perpendicular magnetic field are investigated. Because of the chirality of the Hall edge states, the longitudinal resistances on top and bottom edges of the graphene ribbon are not equal. In the presence of suitable disorder, the top-edge and bottom-edge resistances well show the plateau structures in the both unipolar and bipolar regimes and the plateau values are determined by the Landau filling factors only. These plateau structures are in excellent agreement with the recent experiment. For the unipolar junction, the resistance plateaus emerge in the absence of impurity and they are destroyed by strong disorder. But for the bipolar junction, the resistances are very large without the plateau structures in the clean junction. The disorder can strongly reduce the resistances and leads the formation of the resistance plateaus, due to the mixture of the Hall edge states in virtue of the disorder. In addition, the size effect of the junction on the resistances is studied and some extra resistance plateaus are found in the long graphene junction case. This is explained by the fact that only part of the edge states participate in the full mixing.

PACS numbers: 72.80.Vp, 81.05.ue

I. Introduction

The successful fabrication of graphene, a monolayer of carbon atoms arranged hexagonally,²⁻⁴ had fueled many experimental and theoretical works. For undoped 2-D graphene sheet, Fermi energy is located at the Dirac neutral point. Around the Dirac point, the graphene has a linear dispersion relation, which leads to quasiparticles obeying the massless Dirac-like equation and presents extraordinary properties.⁵⁻⁷ For example, for a graphene under a strong perpendicular magnetic field, its Hall plateaus assume half-integer values,^{3,4,8} $h/[g(n+1/2)e^2]$, where $g = 4$ is the spin and valley degeneracy and n an integer. By varying the gate voltage, both carrier type and concentration of the graphene sheet can be tuned.⁹ A graphene p-n junction is formed by connecting up one p-type graphene and one n-type graphene. Many exciting phenomena closely related to the massless Dirac character of carriers,¹⁰⁻¹⁴ such as relativistic Klein tunneling^{10,11} and Veselago lensing¹², are predicted for graphene p-n junctions.

Recently, the electron transport through the graphene p-n or p-n-p junctions was extensively investigated both experimentally and theoretically.¹⁵⁻¹⁹ In quantum Hall regime, Williams *et al.*¹⁸ experimentally found that the two-terminal conductance exhibits plateaus with half-integer values, $g(|n| + 1/2)e^2/h$, in the case of unipolar junctions and fractional values for bipolar junctions. At about the same time, the theoretical works by Abanin and Levitov¹⁹ explained the appearance of the fractional plateaus by means of the mixture of the electron-like and hole-like Hall edge states in the vicinity of the junction boundary. There were some subsequent investigations on graphene junctions. Using Anderson short-range disorder potentials, Long *et al.*²⁰ and Li *et al.*²¹ numerically com-

puted and analysed the transport behavior of graphene junctions. They found that conductance plateaus emerge in the case of suitable disorder strength. Also, T. Low²² considered the long-range interface and edge disorders in the armchair, zigzag, and antizigzag edge graphene ribbons, and numerically simulated the result of the conductance plateaus.

Very recently, Lohmann *et al.*¹⁷ measured the Hall and longitudinal resistances in a six-terminal graphene junction device. In their experiment, the difference of carrier concentrations between two adjacent regions (the left and right regions) is introduced by chemical doping, and a global gate voltage controls the carrier concentrations in the two regions. By tuning the gate voltage and doping densities, the graphene ribbon can be of p-p, p-n, n-p, or n-n type. They found that Hall resistances of the left and right regions exhibit half-integer plateaus, as usual. Furthermore, the longitudinal resistances also exhibit plateau structures. In particular, the longitudinal resistances at opposite edges are not equal. For instance, with the filling factors $(\nu_L, \nu_R) = (2, -2)$ (here $\nu_{L/R}$ is the Landau filling factor in the left/right region), the longitudinal resistance at one edge is h/e^2 but it is zero at the other edge. By using the concept of the mixture of Hall edge states near the p-n junction boundary, they explained the appearance of these plateaus and the difference between the longitudinal resistances at the opposite edges. So far, there is not any theoretical investigation which gives quantitative and numerical result to explain Lohmann's experimental result. More effort needs to be done in order to find out how disorders affect the resistance plateaus and how the plateaus depend on disorder strength.

In this paper, we theoretically and numerically study

electron transport through graphene junctions. Following the experiment by Lohmann *et al.*, we consider the six-terminal graphene junction device [shown in Fig. 1(a)]. A perpendicular magnetic field B is applied to the graphene sheet. By using the tight-binding Hamiltonian and the Landauer-Büttiker formulism in the framework of non-equilibrium Green's function method, the longitudinal and Hall resistances are calculated. The numerical results show that the longitudinal resistances R_t and R_b of the top and bottom edges, respectively, are usually different in the presence of the magnetic field, as expected from the property of the chirality of Hall edge states. There is an essential difference in the transport behavior between unipolar and bipolar graphene junctions. For unipolar (n-n and p-p) junctions, the longitudinal resistances have plateau structures in the case of clean (no disorder) graphene. The resistance plateaus can keep in the moderate disorder strength, and they are destroyed until the very strong disorder. On the other hand, for bipolar (n-p and p-n) graphene junctions, the longitudinal resistances R_t and R_b are very large in the clean case. But in the presence of disorder, they are strongly decreased even when the disorder strength is weak. For n-p junctions, the top-edge resistance R_t reduces to a moderate positive value, but the bottom-edge resistance R_b drops to zero or even turns negative. In a suitable range of disorder strength, the resistances R_t and R_b of bipolar junctions also have plateau structures due to the full mixing of Hall edge states. For the lowest filling factors, the resistance plateaus exist in a very broad range of disorder strength. Hence, they are produced easily in experiment. But for high filling factors, the plateau only emerges in a narrow disorder range, if it exists. Furthermore, for moderate disorder, the plots of the longitudinal resistances versus the gate voltage exhibit plateau structures in both cases of unipolar and bipolar junctions and the plateau values are only determined by the filling factors (ν_L, ν_R), which are in excellent agreement with the recent experiment by Lohmann *et al.*. In addition, we also find some extra resistance plateaus in long graphene junctions. This is explained by the suggestion that only part of edge states participate in the mixing mechanism.

The rest of the paper is organized as follows. In Section II, we describe the model and give the details of our calculations. In Section III, the numerical results are given. Finally, a brief conclusion is presented in Section IV.

II. Model and calculation

We consider the six-terminal graphene junction device which is illustrated in Fig. 1(a). The six terminals are labelled by the terminal- i ($i = 1, 2, \dots, 6$). Terminals 1 and 4 are the current source and drain, respectively, and other terminals are used as the voltage probes. The whole graphene device is basically divided into three regions: the left, central and right regions as shown in Fig. 1(a). Each of the left and right regions includes three terminals. The dimension of the central region is described by the

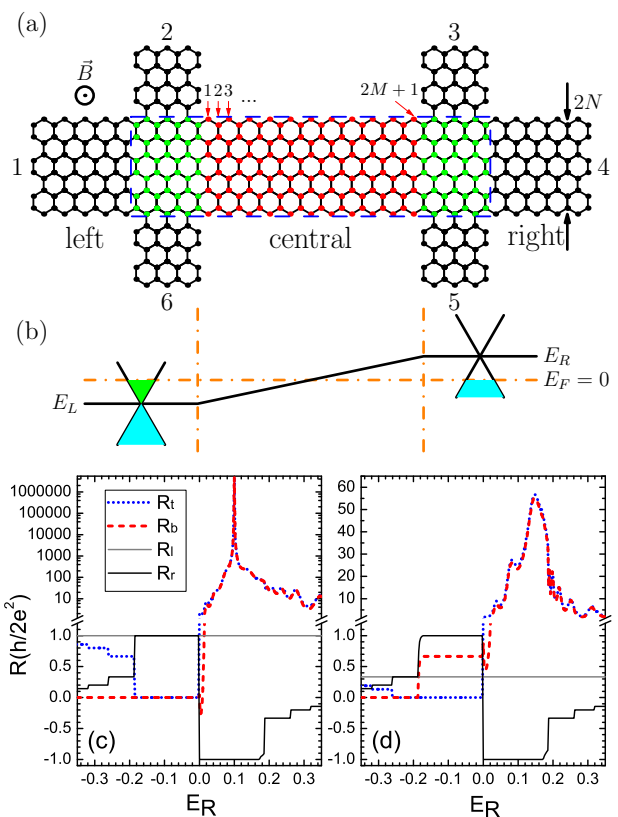


FIG. 1: (Color online) The panel (a) is the schematic diagram for the six-terminal graphene p-n junction device and the panel (b) is for the Dirac energy ϵ_i in the left, central and right regions. The panels (c) and (d) show the resistances vs. E_R at the clean graphene junction ($W = 0$) with $E_L = -0.1$ (c) and -0.2 (d), respectively. The other parameters are the width $N = 50$, the length $M = 20$, and $\phi = 0.01$.

integers N and M [see the red-site (dark gray) region in Fig. 1(a)]. There are totally $2N \times (2M + 1)$ carbon atoms in the central region. The width and length of the central region are $a(3N - 1)$ and $\sqrt{3}a(M + 1)$, respectively. The width of voltage terminals is chosen as $\sqrt{3}aN$, where $a \approx 0.142$ nm is the distance between two neighboring carbons. Fig. 1(a) shows the case $N = 3$ and $M = 10$.

The whole system is subjected to a perpendicular magnetic field which leads to the formation of Landau levels. In quantum Hall regime, bulk states are compressible, and the chiral edge states flow along the edges. This behavior is independent of the type of the edges if the graphene ribbon is wide enough. So we choose wide zigzag-graphene ribbon for our simulation. Compared to the hopping term, both Zeeman splitting and spin-orbit coupling are very small and hence they are negligible. Furthermore, we adopt Anderson on-site disorder. In fact, other types of disorders (e.g. the interface disorder and the long-range disorder) may exist in the experimental device and also lead to the edge state mixing. But from the point of the edge state mixing, these other types

of disorders should have the similar effect. Here we can assume Anderson disorder only exists in the central region based on the fact that the effect of disorder in the left and right regions is suppressed by edge states when the ribbon is wide enough.²³

In the tight-binding representation, the Hamiltonian of the six-terminal graphene junction is given by^{20,21,24}

$$H = \sum_i \epsilon_i a_i^\dagger a_i - \sum_{\langle ij \rangle} (t e^{i\phi_{ij}} a_i^\dagger a_j + h.c.), \quad (1)$$

where a_i^\dagger and a_i are respectively the creation and annihilation operators at site i , and ϵ_i the energy of Dirac point (i.e., the on-site energy). In the left and right regions, ϵ_i is equal to E_L and E_R , respectively [Fig. 1(b)], which can be controlled by the gate voltage in the experiment. In the central region, $\epsilon_i = k(E_R - E_L)/(2M + 2) + E_L + w_i$, where the column index $k = 1, 2, \dots, 2M + 1$ [see Fig. 1(a)] and w_i is the on-site disorder energy. w_i is assumed to be randomly distributed in the range $[-W/2, W/2]$, where W is the disorder strength. The second term in the Hamiltonian stands for the nearest-neighbor hopping. The effect of the magnetic field B is addressed by the phase $\phi_{ij} = \int_i^j \vec{A} \cdot d\vec{l} / \phi_0$ in the hopping interaction Hamiltonian where $\vec{A} = (-By, 0, 0)$ is the vector potential and $\phi_0 = \hbar/e$. The magnetic field B is applied to the whole device (including the six terminals and central region) along the perpendicular direction.

The multi-terminal resistance²⁵ is defined as $R_{ij,kl} = (V_k - V_l)/I_{i \leftarrow j}$, where the contacts i and j are terminals used to draw and input current, and the two contacts k and l are used to measure the voltage difference. We introduce two longitudinal resistances $R_t = R_{14,23}$ (on the top edge) and $R_b = R_{14,65}$ (on the bottom edge) and two Hall resistances $R_l = R_{14,26}$ (in the left region) and $R_r = R_{14,35}$ (in the right region). These four resistances obey the relation,

$$R_t + R_r = R_b + R_l. \quad (2)$$

From the Landauer-Büttiker formula at zero temperature, the current flowing into terminal- i is given by $I_i = (2e^2/h) \sum_{j(\neq i)} T_{ij}(E_F)(V_i - V_j)$.²⁶ Here, $T_{ij}(E_F) = \text{Tr}[\mathbf{\Gamma}_i \mathbf{G}^r \mathbf{\Gamma}_j \mathbf{G}^a]$ ($i, j = 1, 2, \dots, 6$ and $i \neq j$) is the transmission coefficient from terminal- j to terminal- i at Fermi energy E_F , $\mathbf{\Gamma}_i(E_F) = i[\mathbf{\Sigma}_i^r(E_F) - \mathbf{\Sigma}_i^a(E_F)]$ the line width functions, $\mathbf{G}^r(E_F) = [\mathbf{G}^a]^\dagger = 1/[E_F - \mathbf{H}_{cc} - \sum_{i=1}^6 \mathbf{\Sigma}_i^r]$ the retarded and advanced Greens functions, and \mathbf{H}_{cc} the Hamiltonian of the dashed-box region which includes two green-site (light gray) regions and the red-site (dark gray) central region [see Fig. 1(a)]. The retarded self-energy $\mathbf{\Sigma}_i^r(E_F)$ due to the coupling to the terminal- i can be calculated numerically.²⁷ To determine the longitudinal and Hall resistances mentioned above, we applied a bias V across terminal-1 and terminal-4, and the currents in the voltage probes (terminals 2, 3, 5, and 6) are set to zero. Then from the Landauer-Büttiker formula, the voltages V_2, V_3, V_5 and V_6 of the voltage

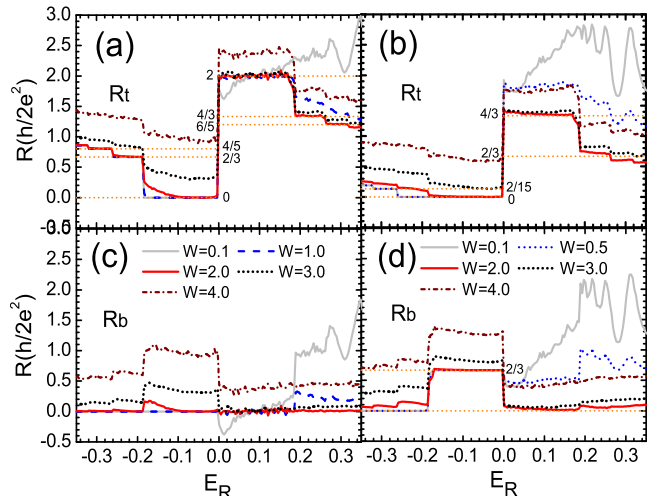


FIG. 2: (Color online) The longitudinal resistances R_t and R_b vs. E_R for the different disorder strength W at the energy $E_L = -0.1$ [panels (a) and (c)] and -0.2 [panels (b) and (d)]. The panels (a) and (b) are for R_t and the panels (c) and (d) are for R_b . The other parameters are the same as in Fig. 1(c) and (d).

probes and the currents I_1 and I_4 can be calculated. We should have $I_1 = -I_4 \equiv I_{14}$. Finally, the longitudinal and Hall resistances are given by $R_t \equiv (V_2 - V_3)/I_{14}$, $R_b \equiv (V_6 - V_5)/I_{14}$, $R_l \equiv (V_2 - V_6)/I_{14}$ and $R_r \equiv (V_3 - V_5)/I_{14}$.

The recursive Green's function technique²⁷ is used for the computation of the transmission coefficient. The Fermi energy E_F is set equal to zero as the energy reference point. The hopping energy $t \approx 2.75$ eV is used as the energy unit, which corresponds to 3×10^4 K. It is reasonable to assume zero temperature condition in our calculations because the temperature in the experiment is only of several Kelvin or sub-Kelvin. Taking into account the spin degeneracy, we will use $h/2e^2$ as the resistance unit. The corresponding filling factors ν_L and ν_R are taken as odd integers ($\pm 1, \pm 3, \pm 5, \dots$) instead of even integers ($\pm 2, \pm 6, \pm 10, \dots$). The effect of the constant magnetic field is addressed by appropriate Peierls phase²⁸: $2\phi \equiv (3\sqrt{3}/2)a^2B/\phi_0$, where $a \approx 0.142$ nm is the distance between two neighboring carbons. We will take $\phi = 0.01$ which corresponds to the magnetic length $l_B = \sqrt{\hbar/(eB)} \approx 1.6$ nm.²⁹ We will consider the case $N = 50$ and $M = 20$, where the area of the central region is 21.2×5.2 nm² and the width of the voltage terminals is 12.3 nm. The reason for using a width of the graphene ribbon far larger than the magnetic length is that edge states can not mix except near the boundary of the junction. Finally, the disorder is averaged over 2000 random configurations except in Fig. 4(a) and (b), where 500 configurations are taken.

III. Numerical results and analysis

We first study the resistances in the clean graphene junction under a strong magnetic field with $\phi = 0.01$. In Fig. 1 (c) and (d), the Hall and longitudinal resistances (R_l , R_r , R_t , and R_b) versus the Dirac energy E_R of the right region are shown. The Dirac energy E_L of the left region is fixed at -0.1 [Fig. 1(c)] or -0.2 [Fig. 1(d)], which corresponds to $\nu_L = 1$ and 3 , respectively. As usual, the Hall resistances R_l and R_r display quantized plateaus with plateau values ± 1 , $\pm 1/3$, $\pm 1/5$, ... [in units of $h/2e^2$], and Hall plateau of a region only depends on the filling factor of the region, $R_l = 1/\nu_L$ and $R_r = 1/\nu_R$. Furthermore, the Hall resistance plateaus are found to be unaffected by the sizes of the central region and the presence of the disorder in the central region, because that the Hall effect is very robust. We will then focus our study on the longitudinal resistances R_t and R_b .

In the presence of the magnetic field, the longitudinal resistance R_t of the top edge usually is not equal to R_b of the bottom edge regardless of the junction type and disorder strength W , because Hall edge states have the chirality which breaks the symmetry of the top and bottom edges. With $E_R < 0$, both R_t and R_b of the clean n-n junction device exhibit perfect plateau structures [Fig. 1(c) and (d)]. By considering the carrier transport along the edges, the plateau values can be analytically obtained:

$$R_t = \left(\frac{1}{|\nu_L|} - \frac{1}{|\nu_R|} \right) \frac{h}{2e^2} \quad \text{and} \quad R_b = 0 \quad (3)$$

for the n-n⁺ regime ($0 < \nu_L \leq \nu_R$) and

$$R_t = 0 \quad \text{and} \quad R_b = \left(\frac{1}{|\nu_R|} - \frac{1}{|\nu_L|} \right) \frac{h}{2e^2} \quad (4)$$

for the n⁺-n regime ($0 < \nu_R \leq \nu_L$). The plateau values can be understood from the following simple argument. It is well known that, for the n-n regime the carriers are electron-like and they move clockwise. For the case $0 < \nu_L \leq \nu_R$ (the n-n⁺ regime), all edge states at the bottom edge are from the right reservoir (i.e. terminal-4), so the voltages V_6, V_5 and V_4 are all equal and this leads to $R_b = (V_6 - V_5)/I_{14} = 0$. According to Eq. (2), R_t is then equal to $(1/|\nu_L| - 1/|\nu_R|)h/2e^2$. The numerical results in Fig. 1(c) and (d) are consistent with the plateau values given in Eqs.(3) and (4). For example, in Fig. 1(c) where $\nu_L = 1$, the resistance R_b is zero and R_t can be equal to 0 , $(2/3)h/2e^2$, $(4/5)h/2e^2$, ... for $\nu_R = 1, 3, 5$, ... And in Fig. 1(d) where $\nu_L = 3$, R_b is 0 or $(2/3)h/2e^2$ and R_t can be 0 , $(2/15)h/2e^2$, $(4/21)h/2e^2$, and so on.

When $E_R > 0$ the device becomes a n-p junction. There is no plateau structure for R_t and R_b , according to Fig. 1(c) and (d). Both R_t and R_b are very large and they are almost equal. Furthermore, the smaller the filling factors are, the larger the longitudinal resistances are. For some values of E_R , R_t and R_b can be over $1000h/2e^2$ (about $13M\Omega$). This is because for the case of clean n-p

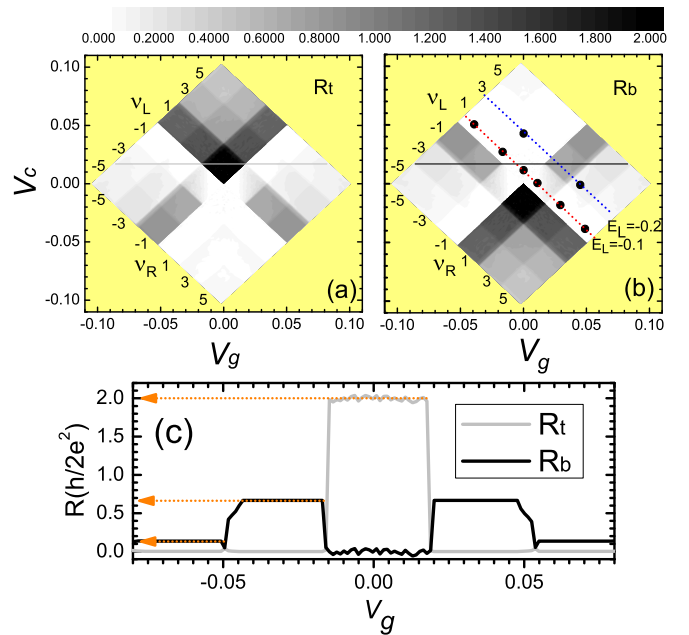


FIG. 3: (Color online) The 2-D plots of the longitudinal resistance R_t (a) and R_b (b) as a function of V_g and V_c , with the parameters $N = 50$, $M = 20$, $W = 2$ and $\phi = 0.01$. (c) The one-dimensional slices shown in (a) (gray solid) and (b) (black solid) are plotted to show the dependency of R_t and R_b on V_g with V_c fixed at 0.015 and $W = 1$.

junction, the edge states in the left and right regions have different chiralities and they are well separated in space. Hence, edge states mixture can not occur and this leads to very large longitudinal resistances.

Next, we shall discuss how R_t and R_b are affected by disorder. Fig. 2 shows the dependence of R_t and R_b on the Dirac energy E_R for different disorder strength W . E_L is fixed at -0.1 ($\nu_L = 1$) or -0.2 ($\nu_L = 3$). For n-n regime ($E_R < 0$), the plateau structures of R_t and R_b still exist for weak and moderate disorder strength. And the plateau values are the same as that of the clean graphene junction. However, in the case of strong disorder (e.g. $W > 3$), R_t and R_b increase and the plateau structures disappear. This is expected as Hall edge states begin to be destroyed by strong disorder. For n-p regime ($E_R > 0$), R_t and R_b are strongly reduced even when the disorder is weak. For example, when $W = 0.1$ (very weak) R_t and R_b are smaller than $3h/2e^2$ for any E_R (Fig. 2), though R_t and R_b can be over $1000h/2e^2$ at some values of E_R for clean junction [Fig. 1(c)]. This significant decrease results from that the electron-like and hole-like Hall edge states start to mix in the vicinity of the n-p interface. It should be obvious from our numerical result that the top-edge and bottom-edge resistances R_t and R_b are not equal and R_b can be negative at some specific values of the parameters [Fig. 2(c)]. For suitable disorder strength, the full edge-state mixture occurs

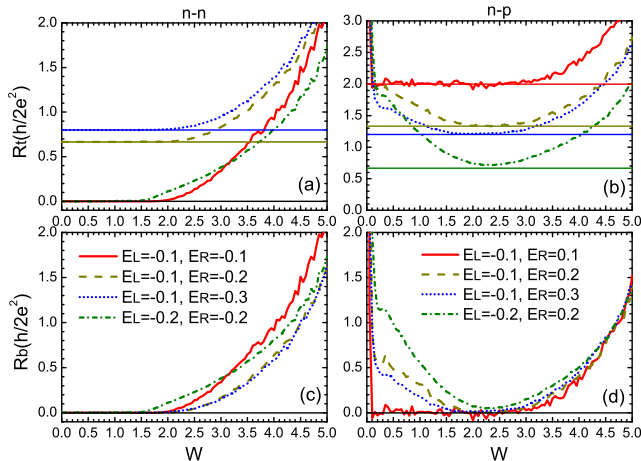


FIG. 4: (Color online) The disorder dependence of longitudinal resistances R_t and R_b with selected (ν_L, ν_R) [which are represented by the solid dots in Fig. 3(b)]. (a) and (b) are for R_t and (c) and (d) are for R_b . The other parameters are the same as in Fig. 1(c).

and hence R_t and R_b exhibit plateau structures (see the curves of $W = 2$ in Fig. 2). According to the Landauer-Büttiker formula under the condition of full edge-state mixture in the central region (junction), the plateau values can be analytically obtained:

$$R_t = \left(\frac{1}{|\nu_L|} + \frac{1}{|\nu_R|} \right) \frac{h}{2e^2} \quad \text{and} \quad R_b = 0. \quad (5)$$

In Fig. 2, the plateau values for some low filling factors (ν_L, ν_R) have been labeled and they are well consistent with the numerical results.

In the following we shall base on our model to simulate the recent experimental results. In Ref. 17, a difference of carrier concentrations between the left and right regions was introduced by chemical doping and a global gate voltage V_g was used to control the carrier concentrations of the whole region. So in our theoretical work, we instead introduce two voltages V_g and V_c to control the carrier concentrations. Let $n_{L/R}$ be the carrier concentration in the left/right region. n_L and n_R are related to V_g and V_c in the following way: $n_L \propto -V_g - V_c$ and $n_R \propto -V_g + V_c$. Because of the linear dispersion relation of graphene, the carrier concentration $n_{L/R}$ is approximately proportional to $\text{sgn}(E_{L/R})E_{L/R}^2$.^{30,31} So we have

$$\text{sgn}(E_L)E_L^2 = \beta(-V_g - V_c), \quad \text{sgn}(E_R)E_R^2 = \beta(-V_g + V_c), \quad (6)$$

where β is a constant. We assign β to be 1 in order to simplify the expressions.

Figs. 3(a) and (b) are the 2-D plots of R_t and R_b as functions of V_g and V_c with the disorder strength $W = 2$. The axes E_L (or ν_L) and E_R (or ν_R) shown in Figs. 3(a) and 3(b) are determined by Eq.(6). The dotted lines in

Fig. 3(b) are identical to the curves plotted in Fig. 2. From the figure we see that R_t and R_b have the following symmetry properties: (i) a mirror symmetry with respect to the line $V_g = 0$

$$R_t(\nu_L, \nu_R) = R_t(-\nu_R, -\nu_L) \quad (7)$$

$$R_b(\nu_L, \nu_R) = R_b(-\nu_R, -\nu_L), \quad (8)$$

which reflects the inversion of the edge-state chiralities; (ii) an inversion symmetry

$$R_t(\nu_L, \nu_R) = R_b(\nu_R, \nu_L) \quad (9)$$

because of the interchange of R_t and R_b by rotating the angle π round the center of the device. Furthermore, both resistances R_t and R_b exhibit the plateaus in the whole space of the parameters V_g and V_c . R_t and R_b are approximately constants at fixed filling factors (ν_L, ν_R) . But as (ν_L, ν_R) varies, the jump of R_t and R_b occurs so that the borders of the filling factors (ν_L, ν_R) are clearly seen in Fig. 3(a) and (b). Here the resistance plateau values in n-n and n-p regimes are coincidental with Eqs.(3), (4) and (5).

In Fig. 3(c), the variations of R_t and R_b along the horizontal solid lines in Fig. 3(a) and (b) are shown. With the range of the gate voltage V_g from -0.1 to 0.1 , the corresponding filling factors (ν_L, ν_R) are $(-3, -5)$, $(-1, -3)$, $(1, -1)$, $(3, 1)$, and $(5, 3)$. The figure shows that in unipolar (n-n and p-p) regime, the top-edge resistance R_t is always equal to zero. But the bottom-edge resistance R_b is $(2/3)h/2e^2$ at $(\nu_L, \nu_R) = (-1, -3)$ and $(3, 1)$, and $(2/15)h/2e^2$ at $(\nu_L, \nu_R) = (-3, -5)$ and $(5, 3)$. For the bipolar (n-p) regime, $(\nu_L, \nu_R) = (1, -1)$, the plateau of R_t is $2h/2e^2$ and R_b is zero. These resistance plateau values are well in agreement with the recent experiment results [see Fig.5(c) in Ref. 17].

The disorder strength dependence of the longitudinal resistances at the selected filling factors (ν_L, ν_R) from Fig. 3(b) (represented by solid dots) is shown in Fig. 4. Because of the relation between R_t and R_b given in Eq. (2), R_t and R_b have similar characteristics with respect to the disorder strength W even though $R_t \neq R_b$. For n-n regime (see the left panels of Fig. 4), R_t and R_b in the clean junction ($W = 0$) have plateau structure. The plateau structure still exists when W increases from zero. However, when W increases beyond a critical value W_c , R_t and R_b start to increase from the plateau values. The critical value W_c is found to be dependent on the filling factors (ν_L, ν_R) : $W_c \approx 2.0$ for $(\nu_L, \nu_R) = (1, 1)$, $(1, 3)$ and $(1, 5)$, and $W_c \approx 1.5$ for $(\nu_L, \nu_R) = (3, 3)$. However, for n-p regime (see the right panels of Fig. 4), R_t and R_b are very large in the clean junction. When W increase from zero, R_t and R_b decrease sharply. For example, when W increases from zero to 0.1, R_t is reduced by two or three orders of magnitude to a finite value, while R_b is reduced to zero. As W continues to increase, both R_t and R_b decrease to certain plateau values. The plateau exists in a certain range of disorder strength, where the full mixing of the electron-like and hole-like edge state

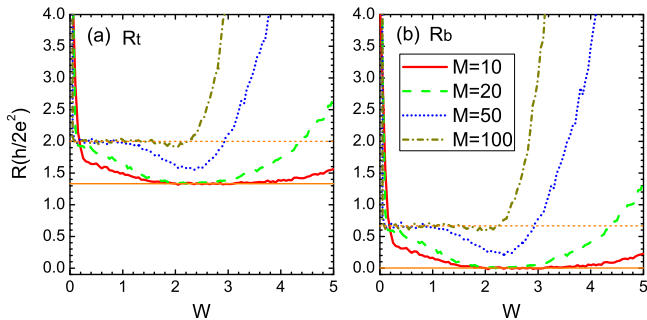


FIG. 5: (Color online) The resistances R_t (a) and R_b (b) vs. the disorder strength W for the different length M of the center region. The parameters are $E_L = -0.1$, $E_R = 0.2$, $\phi = 0.01$, and $N = 50$.

occurs. For the lowest filling factors $(\nu_L, \nu_R) = (1, -1)$, the plateau values $R_t = h/e^2$ and $R_b = 0$ exist in a very broad range of disorder strength, from 0.1 to 3.0. For $(\nu_L, \nu_R) = (1, -3)$ and $(1, -5)$, the disorder range for the existence of resistance plateau are from 1.7 to 2.7 and from 1.9 to 2.7, respectively, which is narrower than that of $(1, -1)$. For higher filling factors [$(\nu_L, \nu_R) = (3, -3)$ or higher], the plateau does not exist, due to the fact that it is more difficult to completely mix all edge states in the case of high filling factors. This means that the resistance plateaus with lower filling factors are easier to be observed in experiment. Finally, when W further increase to be large than 3, R_t and R_b start to increase for all cases of filling factors, which indicates that the edge states are destroyed by strong disorder.

Now we study the size effect of the central region on R_t and R_b . For unipolar graphene junction, the resistances R_t and R_b are almost unaffected by the length M and width N of central region, except for the case of very small N . In the following we focus on the bipolar junction case. Fig. 5 shows the dependence of R_t and R_b on disorder strength W at different length M for the filling factors $(\nu_L, \nu_R) = (1, -3)$. For other filling factors, the results are similar. From Fig. 5, we can see that when the central region is short (e.g. $M = 10$), the full-mixing ideal plateaus [$R_t = (4/3)h/2e^2$ and $R_b = 0$] exist in a wide disorder range $1.6 < W < 4$. This can be understood as the small size of the central region makes the edge states close to each other and hence the full mixing of the states occurs. With increasing length M , the full mixing is more difficult. Under this condition R_t and R_b are enhanced and the corresponding disorder range for the ideal plateaus narrows down or even disappears. For example, for $M = 20$, the ideal plateau exists only in the disorder range $1.7 < W < 2.7$ which is much narrower than that of $M = 10$. For larger M such as 50 and 100, the ideal plateaus do not exist in any case of disorder strength. Although full-mixing plateaus disappear in the case of longer junction, extra plateaus [$R_t = 2h/2e^2$ and $R_b = (2/3)h/2e^2$] emerge in a long enough junction

(e.g. $M = 100$). The existence of the extra plateaus can be explained by the partial mixing of edge states. The assumption of partial mixing of edge states in long enough junctions is reasonable, because part of the Hall edge states are near the junction boundary but the other Hall edge states are far away from the boundary. Let us assume that there are (x_L, x_R) edge states taking part in the full mixing [i.e., the residual $(|\nu_L| - x_L, |\nu_R| - x_R)$ edge states in the left and right regions do not participate in any mixing], the plateau values can be analytically obtained by Landauer-Büttiker formalism:

$$R_t = \left(\frac{1}{x_L} + \frac{1}{x_R}\right) \frac{h}{2e^2}$$

$$R_b = \left(\frac{1}{x_L} + \frac{1}{x_R} - \frac{1}{|\nu_L|} - \frac{1}{|\nu_R|}\right) \frac{h}{2e^2} \quad (10)$$

If $x_L = |\nu_L|$ and $x_R = |\nu_R|$ (i.e. full mixing), the result of Eq.(10) reduces to Eq.(5). By taking $x_L = 1$, $x_R = 1$ and $(\nu_L, \nu_R) = (1, -3)$, the plateau values given by Eq.(10) are $R_t = 2h/2e^2$ and $R_b = (2/3)h/2e^2$, which are well consistent with the numerical results in Fig. 5.

Finally, we simply discuss how the width N of a graphene junction affects R_t and R_b . With increasing N at fixed length M , the resistances R_t and R_b decrease, the resistance plateaus exist in broader disorder range regardless of the type of the junction (unipolar or bipolar). Also, for the large N , some high-filling-factors resistance plateaus emerge. This is expected as Hall edge states in a wider junction have more chance to mix with each other.

IV. Conclusion

In summary, we have investigated the longitudinal resistances at the two edges of a six-terminal graphene junction in the presence of a perpendicular magnetic field. By considering the presence of disorder in the vicinity of the junction interface, the longitudinal resistances at opposite edges exhibit different plateau structures. It is found that the plateau values are only determined by the Landau filling factors. The numerical results are in excellent agreement with the recent experiment by Lohmann *et al.* Furthermore, for unipolar junctions, resistance plateaus exist in clean junctions. The plateau structure can be kept in the presence of weak and moderate disorder, and they are destroyed by very strong disorder. However, for bipolar junctions, the longitudinal resistances are very large and do not have any plateau structure in the clean case. In the presence of disorder, the resistances sharply drop even in the case of very weak disorder and they exhibit plateau structures for suitable disorder strength. In addition, we study the effect of the size of a graphene junction on the resistances and find that some extra resistance plateaus emerge in long graphene junctions. We explain this by proposing that only part of edge states participate in the mixing.

Acknowledgements

This work was financially supported by NSF-China under Grants Nos. 10734110, 10821403, and 10974236 and

China-973 program.

-
- * Email address: sunqf@aphy.iphy.ac.cn
- ² K. S. Novoselov, A. K. Geim, S. V. Morozov, D. Jiang, Y. Zhang, S. V. Dubonos, I. V. Grigorieva, and A. A. Firsov, *Science* **306**, 666 (2004).
 - ³ K. S. Novoselov, A. K. Geim, S. V. Morozov, D. Jiang, M. I. Katsnelson, I. V. Grigorieva, S. V. Dubonos, and A. A. Firsov, *Nature (London)* **438**, 197 (2005).
 - ⁴ Y. Zhang, Y.-W. Tan, H. L. Stormer, and P. Kim, *Nature (London)* **438**, 201 (2005).
 - ⁵ A. H. Castro Neto, F. Guinea, N. M. R. Peres, K. S. Novoselov, and A. K. Geim, *Rev. Mod. Phys.* **81**, 109 (2009).
 - ⁶ C.W.J. Beenakker, *Rev. Mod. Phys.* **80**, 1337 (2008).
 - ⁷ G. W. Semenoff, *Phys. Rev. Lett.* **53**, 2449 (1984).
 - ⁸ A. K. Geim and K. S. Novoselov, *Nature Mat.* **6**, 183 (2007).
 - ⁹ B. Huard, J. A. Sulpizio, N. Stander, K. Todd, B. Yang, and D. Goldhaber-Gordon, *Phys. Rev. Lett.* **98**, 236803 (2007).
 - ¹⁰ M. I. Katsnelson, K. S. Novoselov, and A. K. Geim, *Nature Phys.* **2**, 620 (2006).
 - ¹¹ N. Stander, B. Huard, and D. Goldhaber-Gordon, *Phys. Rev. Lett.* **102**, 026807 (2009).
 - ¹² V. V. Cheianov, V. Fal'ko, and B. L. Altshuler, *Science* **315**, 1252 (2007).
 - ¹³ A. Rycerz, J. Tworzydło, and C. W. J. Beenakker, *Nature Phys.* **3**, 172 (2007).
 - ¹⁴ B. Trauzettel, D. V. Bulaev, D. Loss, and G. Burkard, *Nature Phys.* **3**, 192 (2007).
 - ¹⁵ B. Özyilmaz, P. Jarillo-Herrero, D. Efetov, D. A. Abanin, L. S. Levitov, and P. Kim, *Phys. Rev. Lett.* **99**, 166804 (2007).
 - ¹⁶ D.-K. Ki and H.-J. Lee, *Phys. Rev. B* **79**, 195327 (2009).
 - ¹⁷ T. Lohmann, K. v. Klitzing, and J. H. Smet, *Nano Lett.* **9**, 1973 (2009).
 - ¹⁸ J. R. Williams, L. DiCarlo, and C. M. Marcus, *Science* **317**, 638 (2007).
 - ¹⁹ D. A. Abanin and L. S. Levitov, *Science* **317**, 641 (2007).
 - ²⁰ W. Long, Q.-f. Sun, and J. Wang, *Phys. Rev. Lett.* **101**, 166806 (2008).
 - ²¹ J. Li and S.-Q. Shen, *Phys. Rev. B* **78**, 205308 (2008).
 - ²² T. Low, *Phys. Rev. B* **80**, 205423 (2009).
 - ²³ If the disorder region is extended to the whole dashed-box region, including the red-site (dark gray) central region and two green-site (light gray) regions as shown in Fig. 1(a), the numerical results are almost unchanged. This is because the Hall edge states are robust against the disorder.
 - ²⁴ D. N. Sheng, L. Sheng, and Z. Y. Weng, *Phys. Rev. B* **73**, 233406 (2006).
 - ²⁵ M. Büttiker, *Phys. Rev. B* **38**, 9375 (1988).
 - ²⁶ S. Datta, *Electronic transport in Mesoscopic Systems* (Cambridge University Press, Cambridge, 1995).
 - ²⁷ M. P. L. Sancho, J. M. L. Sancho, and J. Rubio, *J. Phys. F: Met. Phys.* **15**, 851 (1985).
 - ²⁸ A. Cresti, G. Grosso, and G. P. Parravicini, *Phys. Rev. B* **77**, 115408 (2008).
 - ²⁹ $\phi = 0.01$ corresponds $B \approx 250\text{T}$, which is quite a large magnetic field. Due to the small size of the present system, we have to take a strong magnetic field to ensure the magnetic length far smaller than the width of graphene ribbon. For a large system, the magnetic field can be greatly decreased and the numerical results remain the same.
 - ³⁰ A. Cresti, N. Nemeč, B. Biel, G. Niebler, F. Triozon, G. Cuniberti, and S. Roche, *Nano Res.* **1**, 361 (2008).
 - ³¹ Due to the lateral confinement of the system and the presence of the magnetic field, the carrier concentration $n_{L/R}$ is not strictly proportional to $\text{sgn}(E_{L/R})E_{L/R}^2$. But it still is a good approximation because the carrier concentrations $n_{L/R}$ only are the slight fluctuations around $\text{sgn}(E_{L/R})E_{L/R}^2$. In addition, this approximation does not change the value of the resistance plateaus, except for slightly changing the width of the resistance plateaus.